

DESY 01-185

PHYSICS AT HERA II

W. BUCHMÜLLER

Deutsches Elektronen-Synchrotron DESY, 22603 Hamburg, Germany
E-mail: buchmuwi@mail.desy.de

Deep inelastic electron proton scattering at HERA II will allow precise studies of QCD and stringent tests of physics beyond the standard model. We discuss these two aspects of DIS with emphasis on the regime of high gluon densities at small x and on scalar quark production in supersymmetric theories with broken R-parity.

1 Introduction

In deep inelastic scattering at HERA one studies the interactions of electrons with quarks in a wide range of momentum transfers Q^2 and center-of-mass energies $\sqrt{\hat{s}} = \sqrt{xS}$, up to $\sqrt{\hat{s}}_{max} = 318$ GeV. The ‘Virtues of HERA’ have been identified long ago¹. DIS at small Q^2 probes the structure of the proton and allows a variety of QCD tests. DIS at large Q^2 is sensitive to electroweak interactions, to a possible structure of quarks and electrons and, last but not least, to new particles and interactions predicted by extensions of the standard model.

HERA I has made important contributions to all of these topics. The increase of luminosity by a factor of 10 and the availability of longitudinal polarization for electrons and positrons at HERA II will widen the physics scope substantially. In the following we shall illustrate this with some examples concerning strong interactions, electroweak interactions and physics beyond the standard model. This complements the reports of the H1² and ZEUS³ collaborations on their physics program at HERA II. Detailed discussions can be found in the proceedings of previous HERA workshops⁴ as well as in the review articles^{5,6}.

2 Beyond the Standard Model

In connection with the Higgs mechanism of mass generation for vector bosons and fermions new physics beyond the standard model is expected at energies $\mathcal{O}(1 \text{ TeV})$. There are two classes of extensions of the standard model. In the first class a revolutionary change is predicted, either as quark-lepton com-

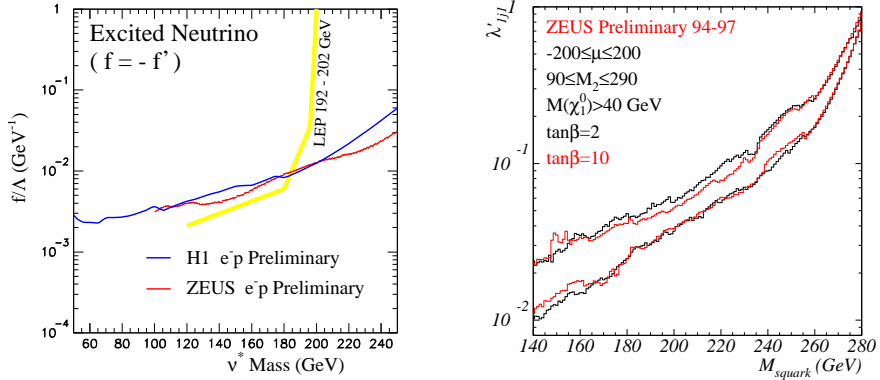


Figure 1. Bounds on coupling versus mass for excited neutrinos⁷ (left), and scalar quarks⁸ (right).

positeness or as manifestations of large extra dimensions. One then expects towers of excitations of the known elementary particles, either excited quarks and leptons or Kaluza-Klein excitations related to the TeV string scale. In the second class of extensions only a ‘mild’ modification of the standard model is predicted, the occurrence of supersymmetry, where each particle acquires a superpartner. These extensions successfully predict the unification of all interactions at the GUT scale $\mathcal{O}(10^{16}$ GeV). Via the seesaw mechanism they can also naturally account for the small neutrino masses indicated by the solar and atmospheric neutrino deficits.

HERA is particularly sensitive to those new particles for which single production is possible in ep-collisions. These include excited quarks and leptons, leptoquarks and scalar quarks in supersymmetric models with broken R-parity. For excited neutrinos the LEP limit of 200 GeV could be significantly extended as shown on the left in fig. (1). On the right the range of upper limits on couplings of scalar quarks is shown as function of the squark mass for a class of supersymmetric models. The Yukawa couplings determine the production cross section, e.g. $\sigma(e_R^+ d_R \rightarrow \tilde{u}_i) \propto \lambda_{1i1}^2$, with $\tilde{u}_1 = \tilde{u}$, $\tilde{u}_2 = \tilde{c}$, $\tilde{u}_3 = \tilde{t}$.

Heavier particles beyond the kinematic reach of HERA lead to effective four-fermion interactions⁹ with strength $4\pi/\Lambda^2$. Depending on the chirality structure lower bounds on Λ up to 9 TeV have been obtained. For the vector-current coupling the bound on Λ can be interpreted as an upper bound on

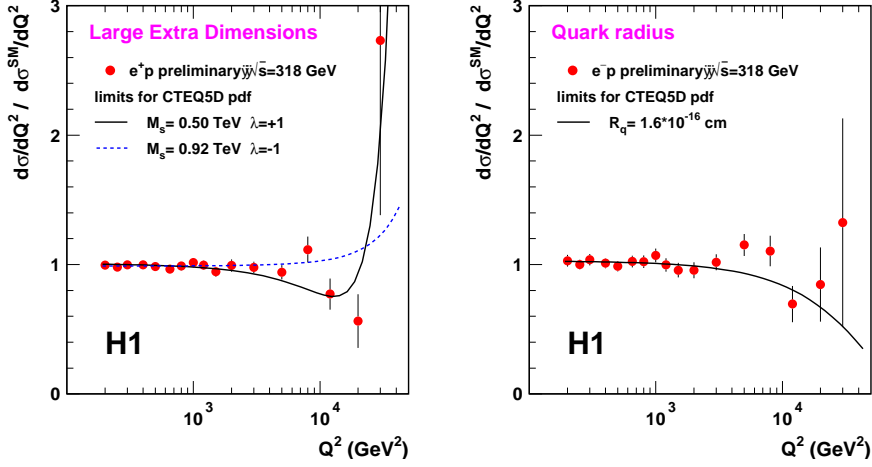


Figure 2. Effect of large extra dimensions of size $\sim 1/M_s$ (left) and of a finite quark radius R_q (right) on the neutral current DIS cross section. From ref.¹⁰.

the electromagnetic quark radius. The present limit is $R_q = 1.6 \times 10^{-16}$ cm (cf. fig. (2)). Contact interactions are also induced by the Kaluza-Klein tower of gravitons in theories with large extra dimensions. The present bound on the corresponding mass scale is about 1 TeV (cf. fig. (2)). At HERA II all these bounds can be improved by about a factor of three.

Supersymmetric theories with broken R-parity are for HERA the most promising extensions of the standard model¹¹. In a class of these models Majorana neutrino masses are generated radiatively. It is then possible to relate the neutrino mixing matrix to squark production cross sections in ep-collisions¹². The analyses of the solar and atmospheric neutrino anomalies favour large neutrino mixings and therefore a neutrino mass matrix of the form

$$m_{\nu ij} = m f_{ij} , \quad (1)$$

where $m < 1$ eV and $f_{ij} = \mathcal{O}(1)$ for all $i, j = 1 \dots 3$. As we shall see, the large mixings among the neutrinos can lead to large couplings of electrons to new particles. The small value of the neutrino mass scale m can be generated radiatively or by mass mixing via the seesaw mechanism.

In the supersymmetric standard model Yukawa interactions are described by the superpotential

$$W = h_{eij} E_i^c L_j H_1 + h_{dij} Q_i D_j^c H_1 + h_{uij} Q_i U_j^c H_2 , \quad (2)$$

where H_1 and H_2 are two Higgs doublets with vacuum expectation values $v_i = \langle H_i \rangle$, $i = 1, 2$, and $v_2/v_1 = \tan \beta$. The fact that the lepton doublets L_i and the Higgs doublet H_1 have the same hypercharge, and therefore identical gauge quantum numbers, motivates the introduction of an additional R-parity violating part of the superpotential,

$$W_R = \frac{1}{2} \lambda_{ijk} L_i L_j E_k^c + \lambda'_{ijk} L_i Q_j D_k^c . \quad (3)$$

The couplings λ and λ' are in principle arbitrary. However, the same reason that leads to the introduction of these R-parity violating couplings also suggests the following connection between λ , λ' and the Yukawa couplings h_e and h_d ,

$$\lambda_{ijk} = \lambda_i h_{eik}^T + \lambda_j h_{eik}^T , \quad \lambda'_{ijk} = \lambda'_i h_{djk} . \quad (4)$$

W_R is then obtained from W by a rotation among the fields (L_i, H_1) . Such a ‘flavour alignment’ suppresses the rates of flavour changing processes in the down quark sector ($\Delta S = 1, 2$, $\Delta B = 1, 2$).

W_R violates lepton number¹³. Hence, Majorana neutrino masses are induced,

$$m_{\nu ij} = \lambda'_i \lambda'_j m_\nu^{(d)} + \lambda_i \lambda_j m_\nu^{(e)} , \quad (5)$$

where $m_\nu^{(d,e)}$ depends on the Yukawa couplings $h_{d,e}$ and the soft supersymmetry breaking parameters. In order to obtain the neutrino mass matrix (2) one needs $\lambda_i, \lambda'_j = \mathcal{O}(1)$. The choice $\lambda_i = \lambda'_j = 1$ leads to the ‘democratic’ mixing matrix.

Predictions of this model with R-parity breaking are certain flavour changing processes, e.g. $BR(D^0 \rightarrow \mu\mu, \mu e) \sim 10^{-5}$ and, in particular, the couplings for squark production, for instance,

$$\lambda'_{111} \sim \frac{m_d}{v} \tan \beta \sim 0.003 , \quad \lambda'_{122} \sim \frac{m_s}{v} \tan \beta \sim 0.05 . \quad (6)$$

The value of λ'_{111} is consistent with the upper bound from neutrinoless double beta-decay. The present upper bound¹⁴ $\lambda'_{122} < 0.29$ based on 37 pb^{-1} suggests that the sensitivity of $\lambda'_{122} \sim 0.05$ will be reached at HERA II.

3 Electroweak Interactions

DIS at large $Q^2 \sim 10^4 \text{ GeV}^2$ has so far tested electroweak unification, i.e., the approximate equality of neutral current and charged current cross section,

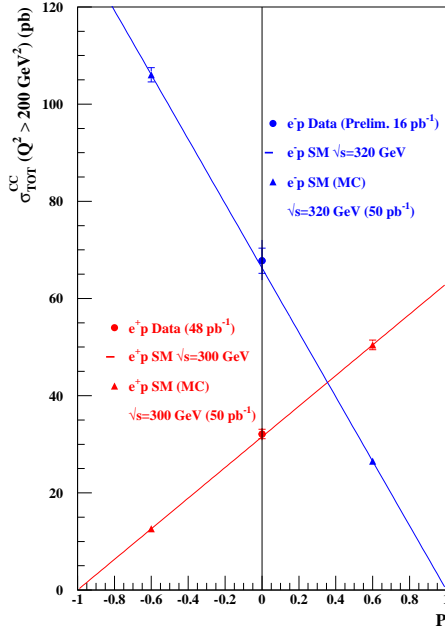


Figure 3. Charged current cross section as function of polarization P . Preliminary ZEUS data for $P = 0$ and Monte Carlo simulations for $P \neq 0$. From ref.¹⁵.

$\sigma(NC) \sim \sigma(CC)$. At HERA II polarization will allow to test the classic prediction of the electroweak theory,

$$\sigma^{CC}(e_R^- p) = \sigma^{CC}(e_L^+ p) = 0 . \quad (7)$$

The exchange of right-handed W_R -bosons leads to a non-zero cross section. One expects a sensitivity to masses $m_{W_R} \simeq 600 \dots 800$ GeV, which corresponds to the present bounds from direct production and electroweak precision tests¹⁶. The expected precision for the charged current cross section obtained after one year of running is shown in fig. (3) as function of the degree of polarisation P .

The weak mixing angle $\sin^2(\theta_W)(M_Z)$ can be determined from a measurement of the polarization asymmetry

$$A(e_L^- - e_R^-) = \frac{d\sigma(e_L^-) - d\sigma(e_R^-)}{d\sigma(e_L^-) + d\sigma(e_R^-)} . \quad (8)$$

For an integrated luminosity of 500 pb^{-1} one expects an error of about 1%¹⁷. This is less accurate, but complementary to the LEP and SLC measurements.

Polarization is also crucial to determine the properties of discovered new particles. For instance, for the scalar quarks discussed in the previous section one has

$$\sigma(e_R^+ p \rightarrow \tilde{c}X) \propto \lambda'_{122}^2, \quad \sigma(e_L^+ p \rightarrow \tilde{c}X) = 0. \quad (9)$$

Such a measurement would prove that the discovered new scalar colour-triplet particle is the superpartner of a left-handed quark.

4 Strong Interactions

In deep inelastic scattering at HERA I many features of QCD have already been studied in great detail. These include

- proton and photon structure functions,
- jets and event shapes,
- determination of α_s ,
- hadronic final states,
- instanton induced processes,
- production of charm and bottom,
- vector meson production,
- diffractive processes.

All these quantities and processes will be studied with higher precision at HERA II, and in particular the search for instanton induced processes¹⁸ will be significantly improved.

In the following I shall concentrate on those aspects which have been most intriguing at HERA I. These are

1. the rapid rise of parton densities at small x ¹⁹, and
2. the large fraction of diffractive events at small x ²⁰.

The rise of the structure functions at small x has been anticipated based on the QCD renormalization group equations for moments²¹ and the corresponding DGLAP evolution equations²² for parton densities in the GRV model²³. In addition, at small x large logarithms $\sim \alpha_s \ln 1/x$ become important and have to be resummed. This is achieved by means of the BFKL

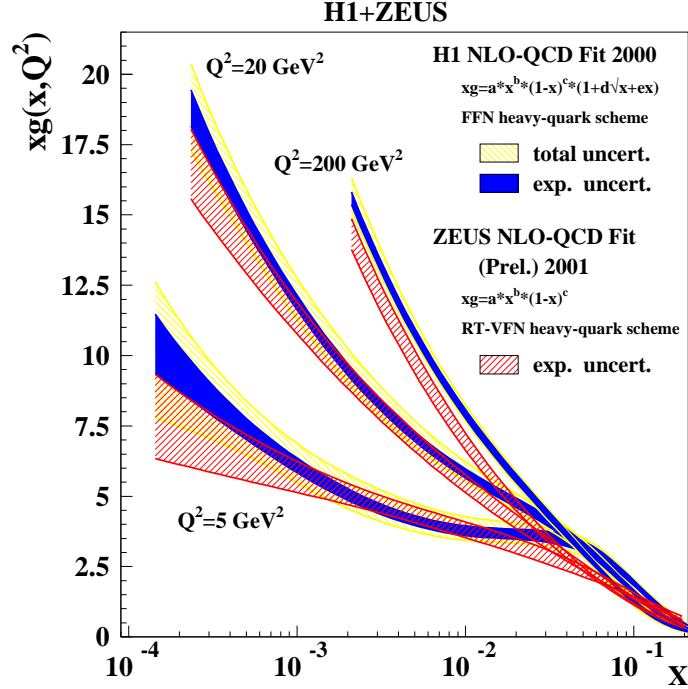


Figure 4. Gluon distribution function determined by a NLO-QCD fit to the structure function $F_2(x, Q^2)$ based on H1 data²⁷ and ZEUS data²⁸, respectively.

equation²⁴ which leads to the prediction of a power-like growth, $F_2 \propto x^{-\lambda}$. The rapid rise at small x reflects the strong radiation of gluons at high energies leading to large gluon densities. However, it still remains to be understood to what extent this rise can be described perturbatively and where it reflects non-perturbative effects, i.e., screening corrections²⁵ and input parton distributions.

In order to identify possible non-perturbative effects, it is important to check how accurately the DGLAP approach describes different processes. A particularly interesting quantity is the gluon density which can be extracted from scaling violations of the structure functions,

$$xg(x, Q^2) \propto \frac{\partial F_2(x, Q^2)}{\partial \ln Q^2} . \quad (10)$$

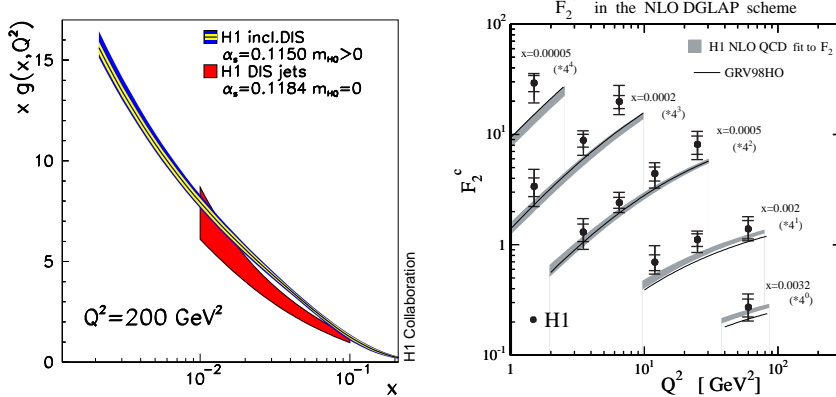


Figure 5. Gluon distribution function extracted from a NLO-QCD fit to dijet rates (left); the charm contribution to F_2 (right).

The gluon density extracted in a NLO analysis from the H1 and ZEUS data is shown in fig. (4) for different values of Q^2 . The related determination of α_s has by now reached the remarkable precision^{29,30},

$$\alpha_s(M_Z^2) = 0.1150 \pm 0.0017(\text{exp}) \pm 0.005(\text{theory}) \text{ (H1)}, \quad (11)$$

$$\alpha_s(M_Z^2) = 0.117 \pm 0.001(\text{stat + uncorr}) \pm 0.005(\text{corr}) \text{ (ZEUS, prel.)}. \quad (12)$$

Note, that the total error of the H1 result is dominated by the theoretical uncertainty.

Contrary to structure functions, the gluon density enters at leading order in the dijet cross section and in F_2^c , the charm contribution to the structure function F_2 . In fig. (5) the NLO gluon density extracted from dijets is compared with the one determined from scaling violations; further, the corresponding prediction for F_2^c is compared with data. It is clear that the higher accuracy at HERA II will lead to a stringent test of the DGLAP framework, which will require NNLO theoretical calculations for structure functions and jet cross sections.

A puzzling phenomenon in DIS at small x is the occurrence of a large fraction $\mathcal{O}(10\%)$ of diffractive events²⁰. This came as a big surprise for most experts in QCD, although it had been anticipated based on Regge theory³¹. However, the large rapidity gap events in DIS are difficult to understand in the parton picture to which almost everybody became used during the past 25 years because of the successes of perturbative QCD.

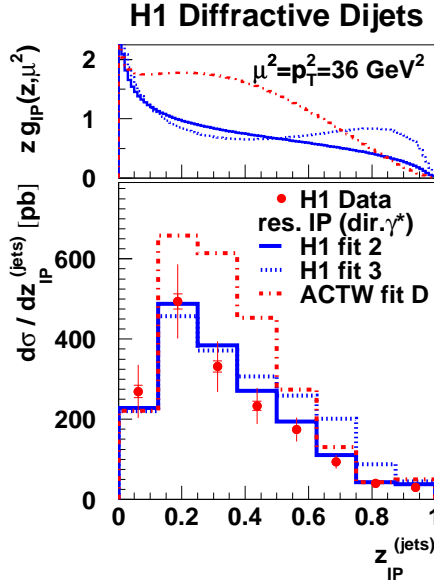


Figure 6. Diffractive dijet cross section as function of $z_P^{(jets)} (= \beta)$, compared with predictions based on different diffractive gluon densities. The corresponding gluon densities $g(z, \mu^2)$ are shown in the upper panel. From ref.³⁷.

We now have learned that, like inclusive structure functions, also diffractive structure functions can be expressed as convolution of parton cross sections with diffractive parton densities^{32,33}. This factorization has been proven for inclusive and diffractive DIS with corresponding rigour³⁴. The variation of the leading twist structure function with Q^2 is given by

$$Q^2 \frac{\partial}{\partial Q^2} F_2^D(\xi, \beta, Q^2) = \sum_q e_q^2 x \frac{\alpha_s}{2\pi} \int_{\beta}^1 \frac{db}{b} \left(P_{qq} \left(\frac{\beta}{b} \right) \frac{dq(b, \xi, \mu^2)}{d\xi} + P_{qg} \left(\frac{\beta}{b} \right) \frac{dg(b, \xi, \mu^2)}{d\xi} \right) . \quad (13)$$

Here $\xi \equiv x_P$ is the fraction of momentum lost by the proton, and $\beta = Q^2/(Q^2 + M^2)$ where M is the diffractive mass, $M^2 = (q + \xi P)^2$. For comparison, in inclusive DIS, $x = Q^2/(Q^2 + W^2)$ where $W^2 = (q + P)^2$ is the total invariant mass squared of the complete hadronic system. $dq/d\xi$ and $dg/d\xi$ are the diffractive quark and gluon densities, respectively, and P_{qq} and P_{qg} are the usual splitting functions. Note, that the Q^2 -evolution affects only the

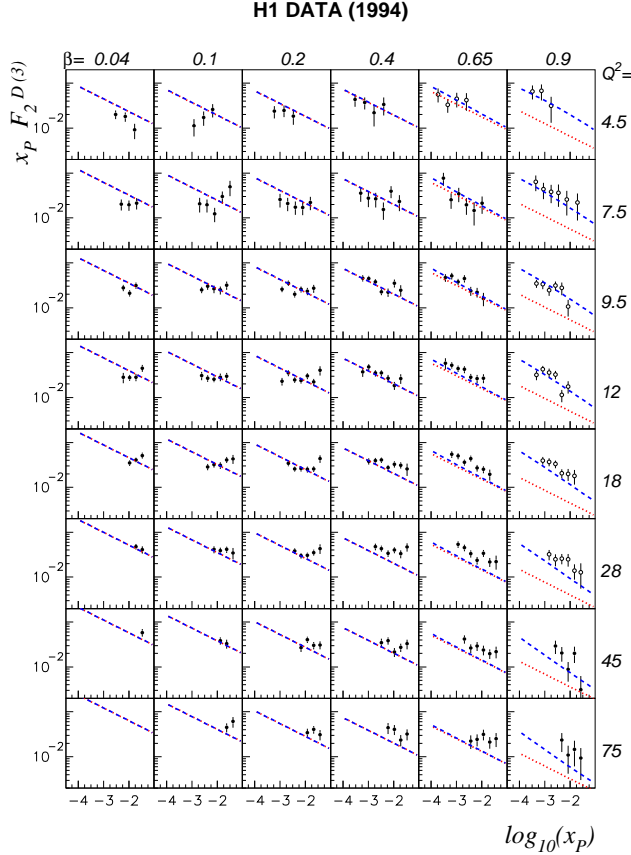


Figure 7. Prediction for the diffractive structure function $x_P F_2^{D(3)}$ compared with H1 data. The dashed lines correspond to the leading twist contribution with the twist-4 component added. The leading twist contribution is shown by the dotted lines. From ref.⁴⁰.

β -dependence of the structure function and not the ξ -dependence. Hence, the ξ -dependence is an entirely non-perturbative property of the proton. It corresponds to the dependence on the total hadronic energy W for fixed β , since $W^2 \simeq Q^2/x = Q^2/(\xi\beta)$. In models with Regge factorization³⁵ the ξ -dependence is given by Regge theory. For the diffractive gluon density one has $dg(\xi, \beta, Q^2)/d\xi \propto \xi^{1-2\alpha_P(0)} g(\beta, Q^2)$.

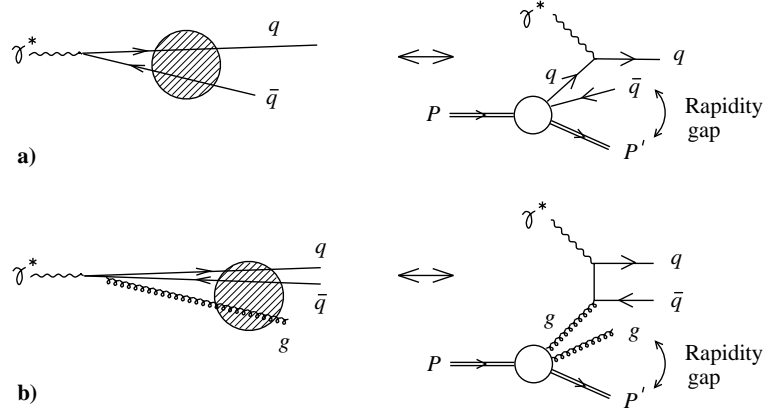


Figure 8. Diffractive DIS in the proton rest frame (left) and the Breit frame (right); asymmetric quark fluctuations correspond to diffractive quark scattering, asymmetric gluon fluctuations to diffractive boson-gluon fusion.

Diffractive DIS can be analyzed in analogy to inclusive DIS³⁶. The diffractive structure function yields the diffractive quark distribution. Its scaling violation, and also diffractive dijet and charm production determine the diffractive gluon density. In fig. (6) the measured dijets rates (lower panel) are compared with predictions based on different diffractive gluon densities $g(z, \mu^2)$ (upper panel) which have been extracted from fits to the diffractive structure function. At present quantitative tests are just beginning. From HERA II we can expect a precise determination of the diffractive gluon density. Here also higher twist effects have to be taken into account at large β ^{38,39}. The results of a recent analysis including such effects are shown in fig. (7).

What do we learn from a determination of diffractive quark and gluon densities? A comparison of inclusive and diffractive DIS is particularly interesting in the proton rest frame⁴¹. Here diffractive and non-diffractive processes can be understood as scattering of partonic fluctuations of the photon on the proton. The diffractive quark and gluon densities then correspond to asymmetric quark and gluon fluctuations (cf. fig. (8)) projected onto the colour singlet state. The formation of the final state is a non-perturbative phenomenon which depends on soft momenta and the properties of confinement. Hence, a comparison of diffractive and non-diffractive processes should help to understand non-perturbative properties of the proton. Correspondingly, one expects that at small x diffractive and non-diffractive processes have a

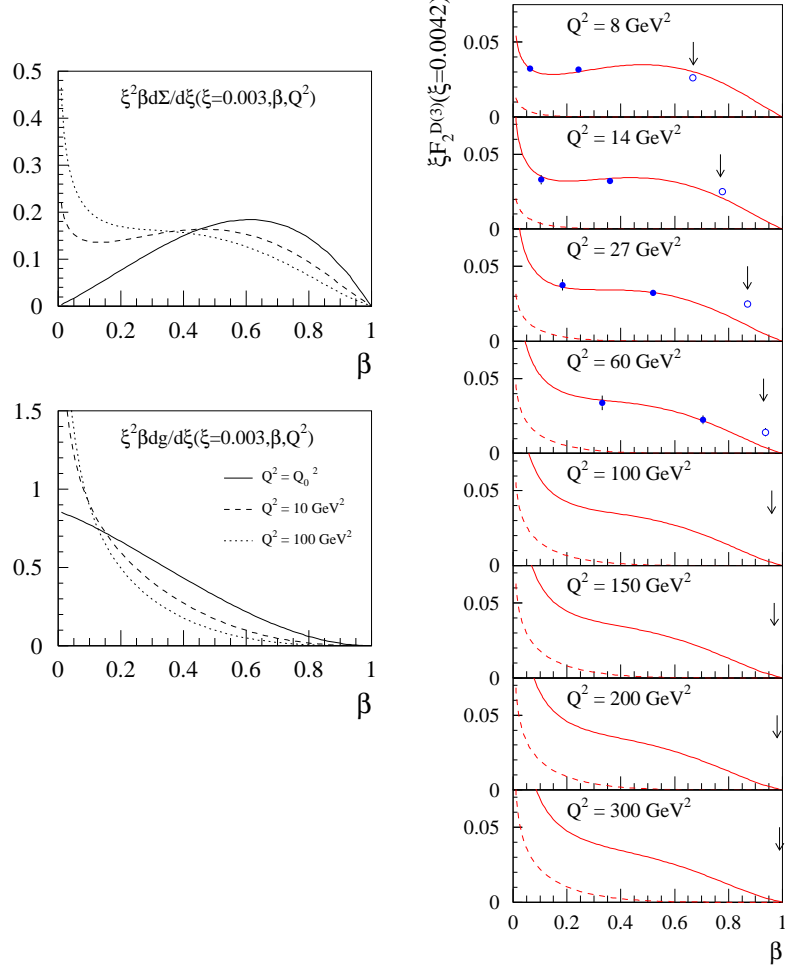


Figure 9. Diffractive singlet quark and gluon distributions at an initial scale Q_0^2 and after Q^2 evolution (left); diffractive structure function $F_2^{D(3)}$ for different values of Q^2 compared with ZEUS data⁴⁹. The arrows indicate the value of β beyond which higher twist terms are expected to become important. From ref.⁴⁶.

similar dependence on the total hadronic energy W ⁴².

An interesting toy model for a comparison of inclusive and diffractive DIS is a large hadronic target^{43,44}. In this model the cross section for a dipole of

transverse size y is of the Glauber-type⁴⁵

$$\sigma(y) = \sigma_0 \left(1 - e^{-ay^2}\right). \quad (14)$$

The corresponding diffractive^{46,40} and inclusive^{46,47} parton densities have been explicitly calculated. The model can also be used to estimate saturation and higher twist effects⁴⁸.

For the diffractive quark and gluon densities one obtains⁴⁶

$$\xi^2 \frac{dq(\beta, \xi, Q_0^2)}{d\xi} = \frac{a\Omega N_c(1-\beta)}{2\pi^3} f_q(\beta), \quad (15)$$

$$\xi^2 \frac{dg(\beta, \xi, Q_0^2)}{d\xi} = \frac{a\Omega N_c^2(1-\beta)^2}{2\pi^3 \beta} f_g(\beta). \quad (16)$$

Here Ω is the transverse size of the target, N_c is the number of colours, and Q_0 is the scale where the model calculation is matched to the perturbative evolution. A non-trivial dependence of the parton densities on $\xi = x_P$ may be introduced by assuming a ξ -dependence either of the transverse size⁴⁶, i.e., $\Omega = \Omega(\xi)$, or of the saturation scale⁴⁰ $a = a(\xi)$, leading to the same phenomenology. Note, that the functions $f_q(\beta)$ and $f_g(\beta)$ are parameter free predictions of the model. The singlet quark density $d\Sigma/d\xi = 6dq/d\xi$ and the gluon density $dg/d\xi$ are shown in fig. (9). Their β -dependence is an interesting non-perturbative property of the proton.

Fig. (9) also shows a comparison between a theoretical prediction⁴⁶ for the diffractive structure function and the presently available ZEUS data⁴⁹. Further data from HERA I and HERA II will allow an extension to larger values of Q^2 where theory predicts almost no change. It will be important to check whether the DGLAP approach is indeed correct for the diffractive structure function. Further, because of the high statistics at HERA II it will be possible to determine the diffractive gluon density also from dijet and charm production. One can then study the non-perturbative dependence on ξ and the normalization relative to the inclusive gluon density. Particularly interesting will be the comparison of event shapes in inclusive and diffractive DIS. In this way we will get for the first time some insight into the regime of high gluon densities in QCD⁵⁰.

5 Summary

The increase in luminosity at HERA II will allow precise measurements of various observables and processes in QCD. Particularly interesting is the determination of α_s , where already now the precision of LEP has almost been

reached. The comparison of the measured running coupling $\alpha_s(\mu^2)$ with lattice calculations will lead to an important quantitative test of QCD. Further, the search for instantons can be improved, and one can test the DGALP framework by comparing determinations of the gluon density from different processes. In this way, HERA can probe the regime of high gluon densities in a clean and controllable way.

The high luminosity and polarization will also lead to new tests of the electroweak theory. Searches for physics beyond the standard model will be significantly improved, in particular with respect to scalar quark production in models with R-parity breaking. Clearly, this sensitivity will also allow the discovery of phenomena not anticipated in this contribution.

Acknowledgments

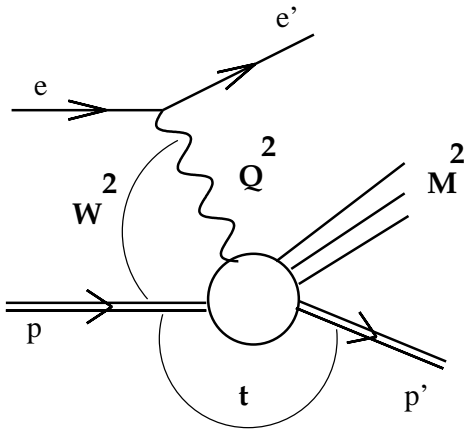
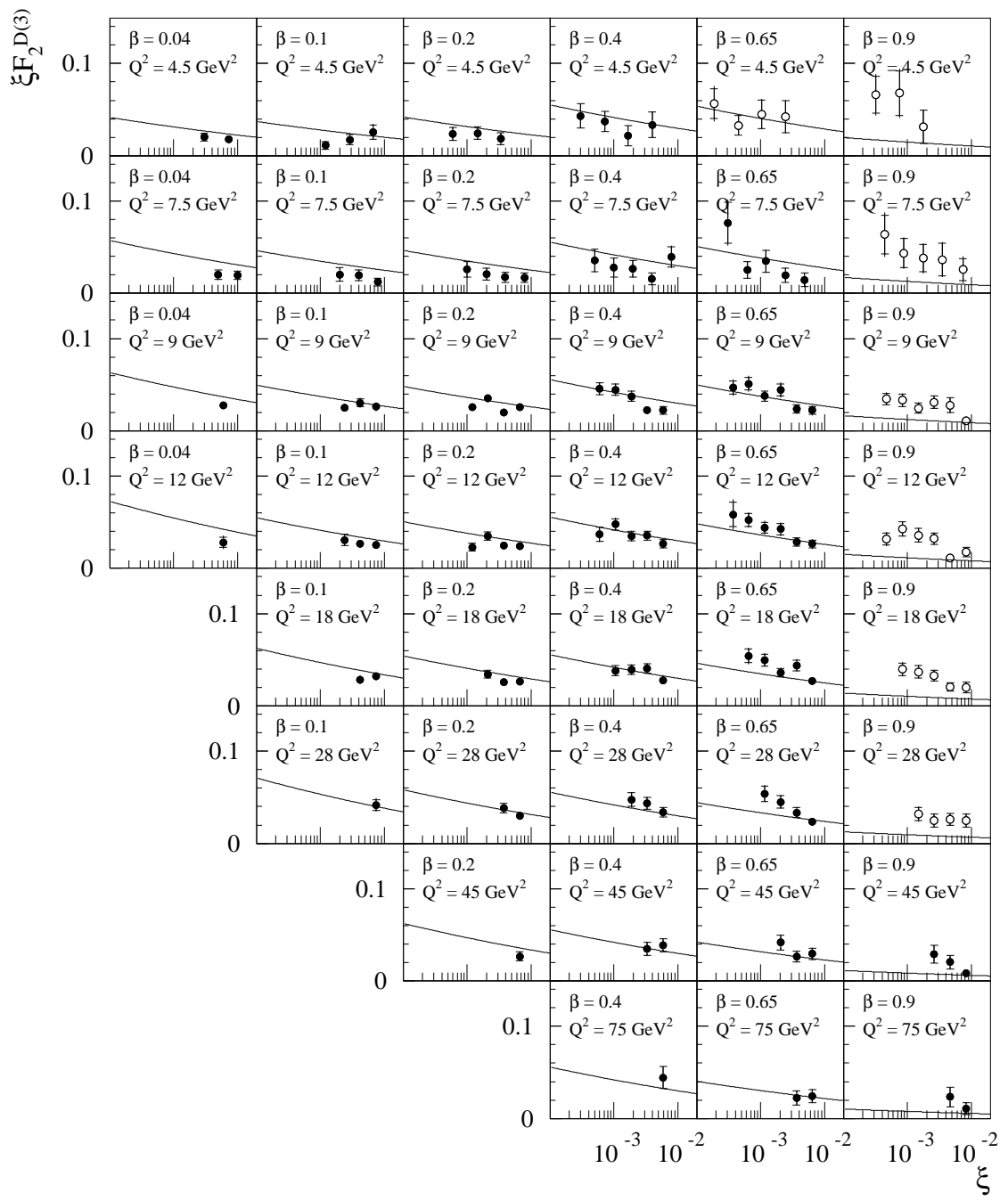
I would like to thank T. Gehrmann, K. Golec-Biernat, D. Haidt, M. Klein, M. Kuze, P. Schleper and G. Wolf for their help in the preparation of this contribution and the organizers of DIS2001 for the splendid hospitality in Bologna.

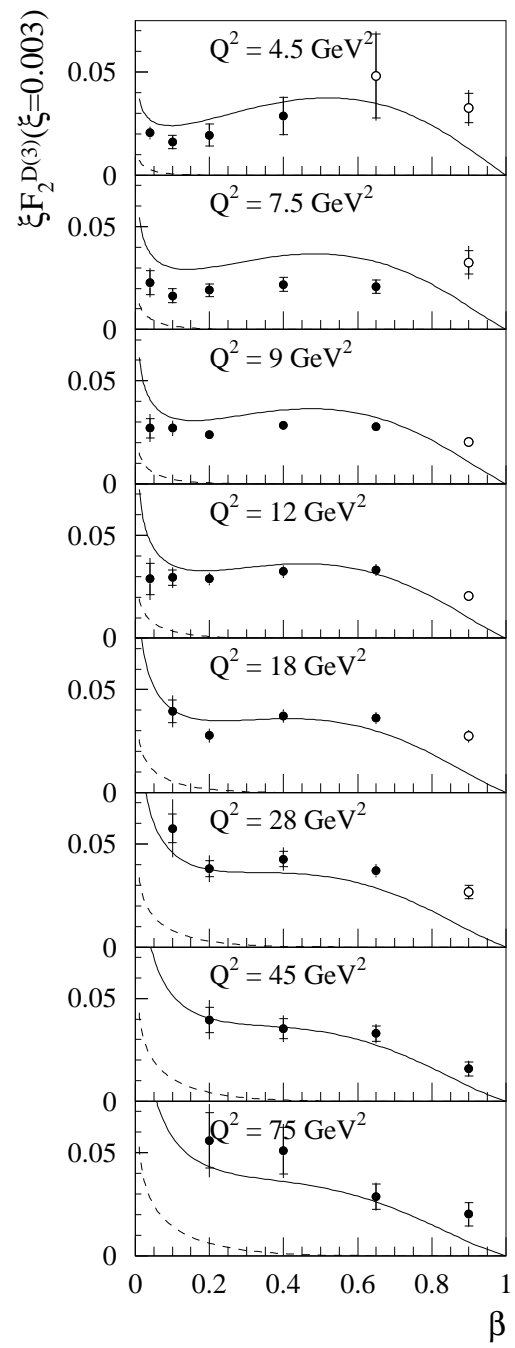
References

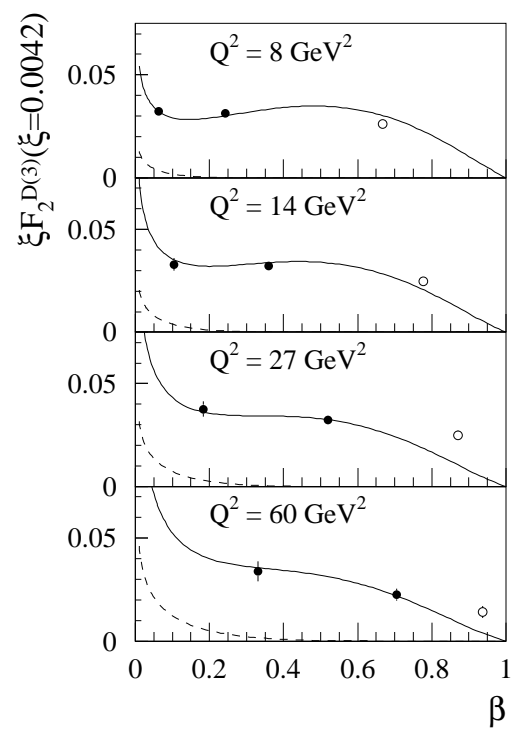
1. L. Maiani, *The Virtues of HERA*, in Proc. *Experimentation at HERA*, Amsterdam 1983, DESY HERA 83/20
2. E. Elsen, these proceedings
3. B. Foster, these proceedings
4. Proc. *The HERA Workshop*, Vol. I,II, Hamburg 1987, ed. R. D. Peccei; Proc. *Physics at HERA*, Vol. I,II,III, Hamburg 1991, eds. W. Buchmüller, G. Ingelman; Proc. *Future Physics at HERA*, Hamburg 1996, eds. G. Ingelman, A. De Roeck, R. Klanner
5. H. Abramowicz, A. Caldwell, Rev. Mod. Phys. **71** (1999) 1275
6. G. Wolf, hep-ex/0105055
7. H1 Collaboration, Paper 956 submitted to ICHEP 2000, Osaka, Japan
ZEUS Collaboration, Paper 1040 submitted to ICHEP 2000, Osaka, Japan
8. ZEUS collaboration, abstract 1042, submitted to ICHEP00, Osaka
9. For a recent review and references, see
M. Kuze, *Searches for new physics at HERA*, hep-ex/0106030
10. H1 Collaboration, C. Adloff et al., Phys. Lett. **B 479** (2000) 358;
H1 Collaboration, Abstract 951 submitted to ICHEP00, Osaka, Japan

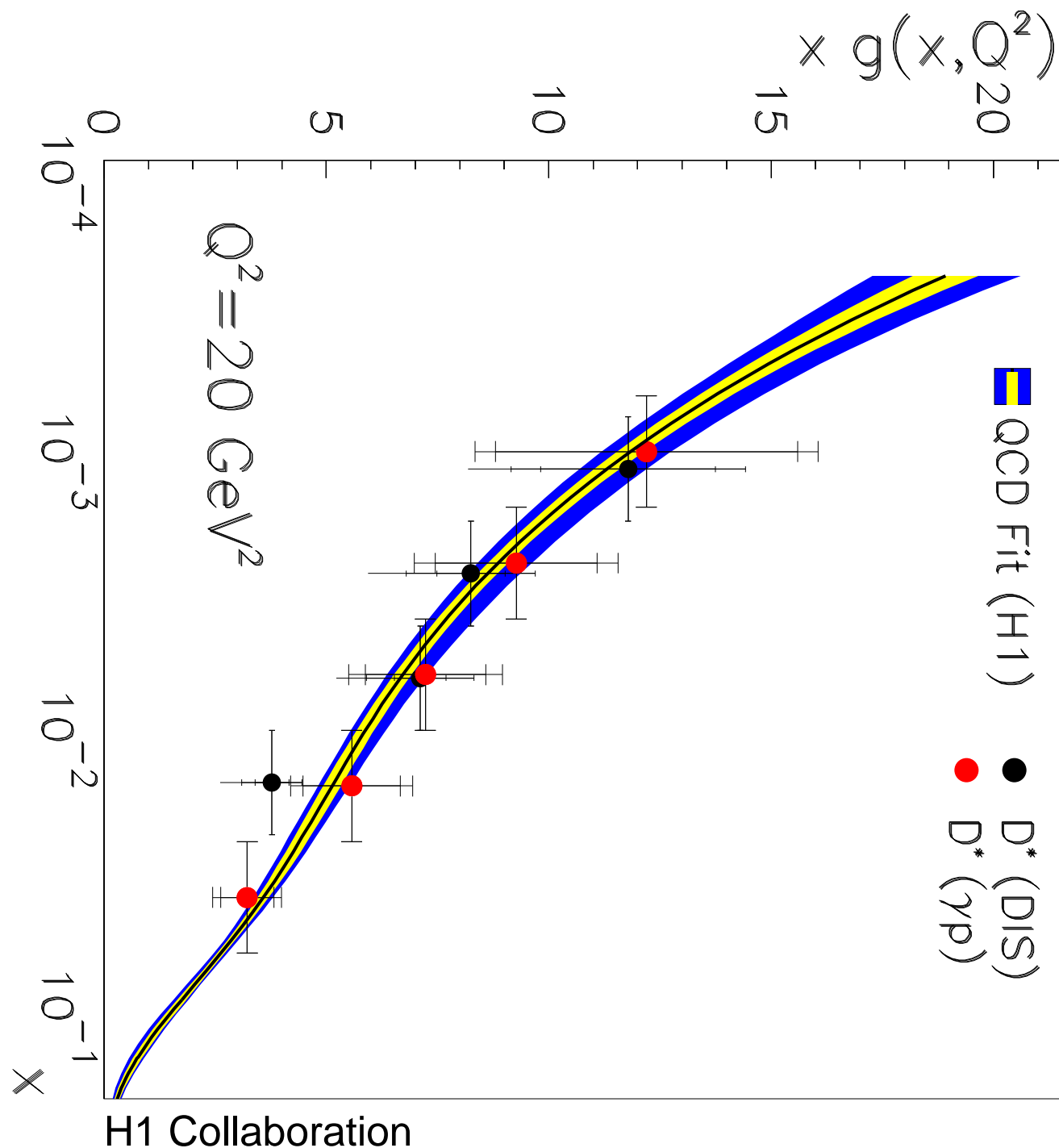
11. E. Perez, Y. Sirois, H. Dreiner, Proc. *Future Physics at HERA*, Hamburg 1996, eds. G. Ingelman, A. De Roeck, R. Klanner, p. 297
12. W. Buchmüller, R. Rückl, in preparation
13. For a recent discussion and references, see
 - A. de Gouvêa, S. Lola, K. Tobe, Phys. Rev. **D 63** (2001) 035004
14. H1 Collaboration, C. Adloff et al., Eur. Phys. J. **C 20** (2001) 639
15. T. Fusayasu, Moriond Conf. on *Electroweak Interactions*, Les Arcs, 2001
16. Review of Particle Physics, Eur. Phys. J. **C 15** (2000) 1
17. J. Blümlein, M. Klein, T. Riemann, in Proc. *The HERA Workshop*, Vol. II, Hamburg 1987, ed. R. D. Peccei, p.687;
D. Haidt, private communication
18. A. Ringwald, F. Schrempp, Phys. Lett. **B 503** (2001) 331
19. H1 Collaboration, I. Abt et al., Nucl. Phys. **B 407** (1993) 515;
ZEUS Collaboration, M. Derrick et al., Phys. Lett. **B 316** (1993) 412
20. ZEUS Collaboratin, M. Derrick et al., Phys. Lett. **B 315** (1993) 481;
H1 Collaboration, T. Ahmed et al., Nucl. Phys. **B 429** (1994) 477
21. A. de Rujula et al., Phys. Rev. **D 10** (1974) 1649
22. V. N. Gribov, L. N. Lipatov, Sov. J. Nucl. Phys. **15** (1972) 438, 675;
G. Altarelli, G. Parisi, Nucl. Phys. **B 126** (1977) 298;
Yu. L. Dokshitzer, Sov. Phys. JETP **46** (1977) 641
23. M. Glück, E. Reya, A. Vogt, Phys. Lett. **306 B** (1993) 391
24. L. N. Lipatov, Sov. J. Nucl. Phys. **23** (1976) 338;
V. S. Fadin, E. A. Kuraev, L. N. Lipatov, Phys. Lett. **60 B** (1975) 50;
Sov. Phys. JETP **44** (1976) 443; *ibid.* **45** (1977) 199;
Y. Y. Balitski, L. N. Lipatov, Sov. J. Nucl. Phys. **28** (1978) 822
25. L. V. Gribov, E. M. Levin, M. G. Ryskin, Phys. Rep. **100** (1993) 481;
for a review and references, see
A. H. Mueller, Proc. *QCD: Perturbative or nonperturbative?*, Autumn School Lisbon 1999, hep-ph/9911289
26. For a recent discussion and references, see
G. Altarelli, R. Ball, S. Forte, Nucl. Phys. **B 599** (2001) 383
27. H1 Collaboration, R. Wallny, these proceedings
28. ZEUS Collaboration, K. Nagano, these proceedings
29. H1 Collaboration, C. Adloff et al., Eur. Phys. J. **C 21** (2001) 33
30. ZEUS Collaboration, A. Cooper-Sarkar, these proceedings
31. A. Donnachie, P. V. Landshoff, Phys. Lett. **B 191** (1987) 309
32. L. Trentadue, G. Veneziano, Phys. Lett. **B 323** (1994) 201
33. A. Berera, D. E. Soper, Phys. Rev. **D 50** (1994) 4328
34. J. C. Collins, Phys. Rev. **D 57** (1998) 3051
35. G. Ingelman, P. E. Schlein, Phys. Lett. **B 152** (1985) 256

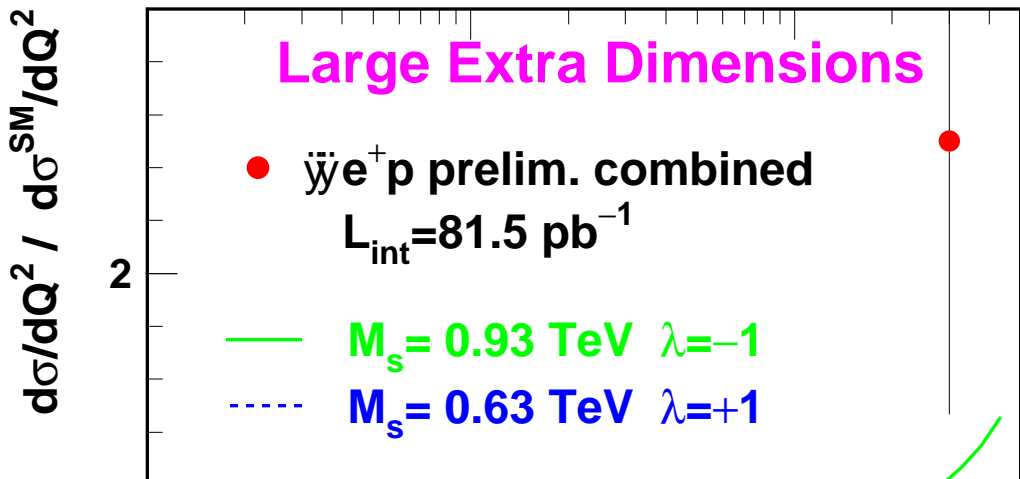
36. T. Gehrman, W. J. Stirling, Z. Phys. **C 70** (1996) 89
37. H1 Collaboration, C. Adloff et al., Eur. Phys. J. **C 20** (2001) 29
38. J. Bartels, J. Ellis, H. Kowalski, M. Wüsthoff, Eur. Phys. J. **C 7** (1999) 443
39. A. Hebecker, T. Teubner, Phys. Lett. **B 498** (2001) 16
40. K. Golec-Biernat, M. Wüsthoff, Eur. Phys. J. **C 20** (2001) 313
41. J. D. Bjorken, AIP Conf. Proc. No.6, eds. M. Bander et al. (AIP, New York, 1972) p. 151;
J. D. Bjorken, J. B. Kogut, Phys. Rev. **D 8** (1973) 1341
42. W. Buchmüller, A. Hebecker, Nucl. Phys. **B 476** (1996) 203;
W. Buchmüller, Phys. Lett. **B 353** (1995) 335
43. L. McLerran, R. Venugopalan, Phys. Rev. **D 49** (1994) 2233
44. A. Hebecker, H. Weigert, Phys. Lett. **B 432** (1998) 215
45. N. N. Nikolaev, B. G. Zakharov, Z. Phys. **C 49** (1991) 607
46. W. Buchmüller, T. Gehrman, A. Hebecker, Nucl. Phys. **B 537** (1999) 477
47. A. H. Mueller, Nucl. Phys. **B 558** (1999) 285
48. K. Golec-Biernat, M. Wüsthoff, Phys. Rev. **D 59** (1999) 014017; *ibid.* Phys. Rev. **D 60** (1999) 114023
49. ZEUS Collaboration, J. Breitweg et al., Eur. Phys. J. **C 6** (1999) 43
50. J. Jalilian Marian, A. Kovner, A. Leonidov, H. Weigert, Nucl. Phys. **B 504** (1997) 415;
A. Kovner, J. G. Milhano, H. Weigert, Phys. Rev. **D 62** (2000) 114005



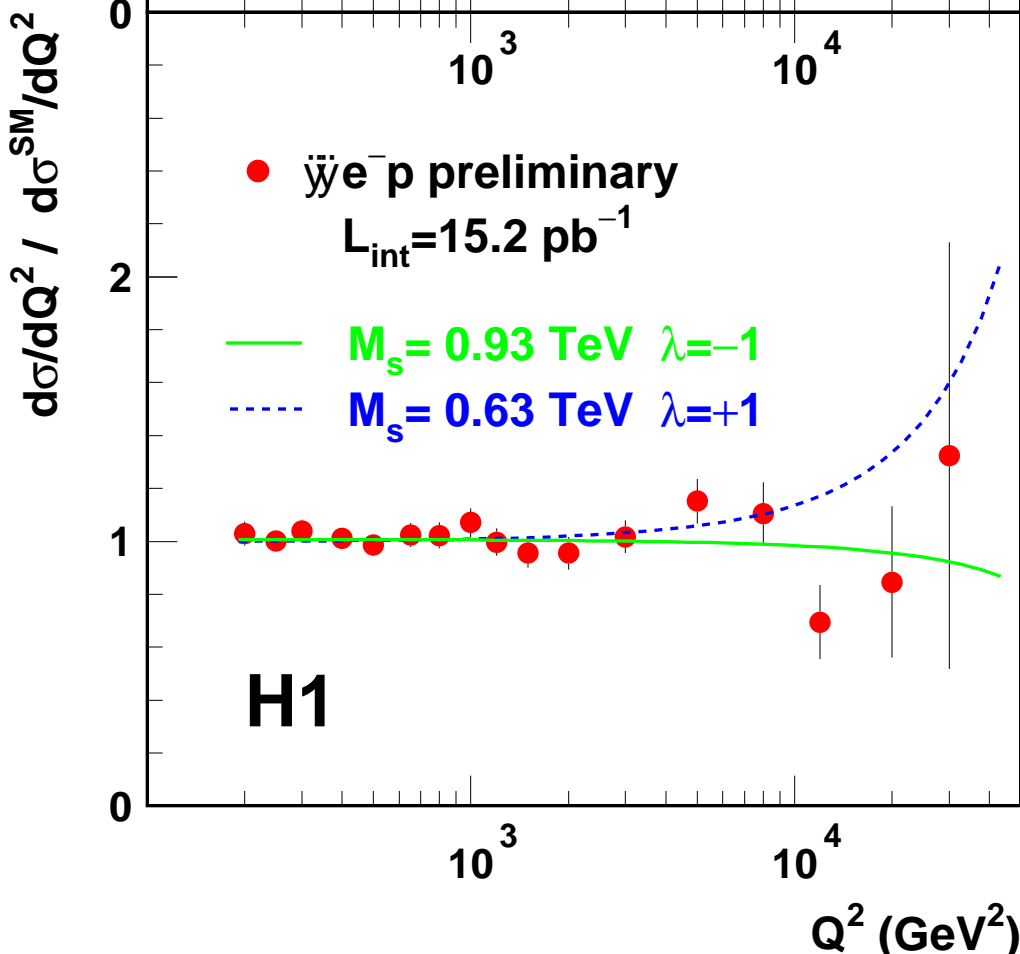








H1



H1

